UC Office of the President
Recent Work

Title
Contortrostatin, a dimeric disintegrin from Agkistrodon contortrix contortrix, inhibits angiogenesis

Permalink
https://escholarship.org/uc/item/7rw102th

Authors
Zhou, Qing
Nakada, Marian T, Centocor
Arnold, Catherine
et al.

Publication Date
1999-09-01

DOI
10.1023/a:1009059210733

Peer reviewed

eScholarship.org Powered by the California Digital Library
University of California

Angiogenesis **3**: 259–269, 1999.
© 2000 *Kluwer Academic Publishers. Printed in the Netherlands.*

Original article

Contortrostatin, a dimeric disintegrin from *Agkistrodon contortrix contortrix*, inhibits angiogenesis

Qing Zhou[1], Marian T. Nakada[2], Catherine Arnold[1], Kate Y. Shieh[1] & Francis S. Markland, Jr[1]
[1]*Department of Biochemistry & Molecular Biology and Norris Comprehensive Cancer Center, University of Southern California, Keck School of Medicine, Los Angeles, California, USA;* [2]*Centocor, 200 Great Valley Parkway, Malvern, Pennsylvania, USA*

Received 14 October 1999; accepted in revised form 29 February 2000

Key words: angiogenesis, disintegrin, integrin, vitronectin receptor

Abstract

Contortrostatin, a 13.5 kDa disulfide-linked homodimeric polypeptide possessing an Arg–Gly–Asp sequence, was isolated from venom of the southern copperhead snake. Daily injection of contortrostatin into the primary tumor of human breast cancer MDA-MB-435 carried in nude mice significantly inhibited tumor growth and neovascularization of the tumor tissue. On the chick embryo chorioallantoic membrane, contortrostatin inhibited angiogenesis induced by MDA-MB-435 cells, basic fibroblast growth factor, and vascular endothelial growth factor. In addition, contortrostatin effectively blocked adhesion of human umbilical vein endothelial cells (HUVEC) to immobilized vitronectin and significantly inhibited invasion of HUVEC through a Matrigel barrier. Competitive binding assays and adhesion assays with different integrin antibodies suggested that integrin $\alpha v\beta 3$ is a binding site for contortrostatin on vascular endothelial cells. Detachment of HUVEC from vitronectin by contortrostatin induced apoptosis. HUVEC adhered and spread well on immobilized contortrostatin without undergoing apoptosis, suggesting that it is the inhibition of adhesion and spreading of HUVEC on extracellular matrix proteins, rather than binding of contortrostatin to integrins *per se*, that triggers apoptosis. We conclude that contortrostatin binds to $\alpha v\beta 3$, and interferes with the anchorage-dependent survival mechanism of the vascular endothelial cells, and the mobility of the cells. The consequent suppression of angiogenesis is an important component of the antineoplastic activity of contortrostatin.

Introduction

It is well established that the growth of a tumor depends on persistent neovascularization [1, 2]. Since the initial report of this hypothesis by Folkman, many angiogenic inducers and inhibitors have been identified (reviewed in [3]). It is believed that the balance of inhibitors and inducers governs the angiogenic switch of the cancer cell [4]. Experimental evidence indicates that tumor growth is proportional to the extent of angiogenesis; inhibition of angiogenesis causes tumor regression [5–7]. Cancer induced angiogenesis is characterized by immature, highly permeable blood vessels that have a discontinuous basement membrane and fewer intercellular junctional complexes than normal mature vessels [8]. Therefore, the angiogenic vessels provide an efficient route for tumor cells to escape from the primary site and enter the blood circulation. It has been reported that vascular density in the tumor is directly correlated with the likelihood of metastasis in human breast cancer patients [9], and vascular density is presently being used as an prognostic variable in breast cancer. Due to the importance of angiogenesis in tumor growth and metastasis, attention has turned to the discovery of angiogenic inhibitors that may have potential usefulness as anti-tumor agents.

Recently, the role of integrins in angiogenesis has been investigated (reviewed in [10]). It has been demonstrated that $\alpha v\beta 3$ undergoes upregulation in endothelial cells during vasculogenesis [11], wound healing [12], and angiogenesis [7, 13]. A monoclonal antibody (mAb) to integrin $\alpha v\beta 3$, as well as a cyclic Arg–Gly–Asp (RGD)-containing peptide, perturbed angiogenesis and produced regression of human breast cancer growing on the chick embryo chorioallantoic membrane (CAM) [7, 13]. Antagonists of $\alpha v\beta 3$ apparently cause apoptosis of vascular endothelial cells which results from the activation of p53 and increase of *bcl*-2/bax ratio [14–16].

Correspondence to: Dr Francis S. Markland, Cancer Research Laboratory, Rm. 106, University of Southern California, Keck School of Medicine, 1303 N. Mission Road, Los Angeles, CA 90033, USA. Tel: +1-323-224-7981; Fax: +1-323-224-7679; E-mail: markland@hsc.usc.edu

Disintegrins are a family of polypeptides found in the venom of vipers and pit vipers. All disintegrins contain an RGD sequence that is essential to their ability to obstruct integrin functions [17]. Several disintegrins have been shown to block the adhesion of human umbilical vein endothelial cells (HUVEC) to vitronectin [18]. Recently, three disintegrins, triflavin, accutin and salmosin were found to have anti-angiogenic activity [19–21]. We have isolated a 13.5 kDa disintegrin, contortrostatin, from southern copperhead snake venom [22, 23]. Unlike other disintegrins, contortrostatin is a homodimer. There is an RGD site in each of the subunits, and this imbues contortrostatin with unique activities compared to monomeric disintegrins [24]. In this report, we show that contortrostatin is an antagonist of $\alpha v\beta 3$, and has a potent inhibitory effect on angiogenesis both *in vitro* and *in vivo*.

Materials and methods

Materials. Venom of *Agkistrodon contortrix contortrix* was purchased from Biotoxins, Inc. (St. Cloud, Florida). Contortrostatin was purified by multistep high performance liquid chromatography (HPLC) according to an established protocol [22, 23]. Vitronectin, fibronectin, Matrigel, basic fibroblast growth factor (bFGF), and vascular endothelial growth factor (VEGF) were purchased from Becton Dickinson (Bedford, Massachusetts). LM609 was a gift from Dr David A. Cheresh (Scripps Research Institute, La Jolla, California). Antibodies 7E3, ^{125}I-c7E3 Fab, and 10E5 as well as purified integrins $\alpha IIb\beta 3$ and $\alpha v\beta 3$ were kindly provided by Centocor (Malvern, Pennsylvania). Goat anti-mouse IgG conjugated with fluorescein isothiocyanate (FITC) was purchased from Jackson ImmunoResearch (West Grove, Pennsylvania). The monoclonal antibody against Factor VIII related antigen and Immunohistochemistry detection kit (HistMouse-SP Kit) were purchased from Zymed Laboratories, Inc. (South San Francisco, California).

Cell culture. Frozen HUVEC were obtained from Dr Florence Hofman (Department of Pathology, University of Southern California). The cells were seeded in 1% gelatin coated tissue culture flask in RPMI-1640 medium containing 2 mM L-glutamine, 20% fetal bovine serum (FBS), 0.1 mg/ml EndoGro (VEC Technology, Inc., New York), 1% Nutridoma HU (Boehringer Mannheim, Indianapolis, Indiana), 20 units/ml heparin, 100 units/ml penicillin, 100 μg/ml streptomycin, and 2.5 μg/ml Fungizone. Cells were used between passage 4 and 7. MDA-MB-435 human breast cancer cells were a gift from Dr Janet Price (MD Anderson Cancer Center, Houston, Texas). Cells were cultured in Minimum Essential Medium containing 10% FBS, 2 mM L-glutamine, 1 mM sodium pyruvate, and penicillin/streptomycin. Subconfluent cells were harvested by trypsinization for experimental use. All cells were incubated in a 37 °C incubator with 5% CO_2.

Nude mouse model of human breast cancer. For the humane treatment of experimental animals, a protocol approved by the Institutional Animal Care and Use Committee, University of Southern California was strictly followed. Female nude mice (BALB/c/nu/nu) at 4-weeks of age were purchased from Simonsen Lab (Gilroy, California). Animals were kept in a pathogen-free environment, and fed sterilized food and water. The orthotopic xenograft nude mouse model was established according to Price et al. [25]. All procedures were performed with aseptic techniques. Nude mice were anesthetized by inhalation of Metofane (Pitman-Moore, Mundelein, Illinois) in a closed chamber. The mammary fat pad under the second nipple from the rostral side was selected for implantation of cancer cells. A longitudinal incision of 1 cm was made on the lateral side of the nipple where the mammary fat tissue beneath the skin was carefully exposed. MDA-MB-435 cells (5×10^5) resuspended in 0.1 ml PBS were injected into the mammary fat pad. The wound was then sutured. Palpable tumor masses appeared 10 days post-implantation. At that time the mice were randomized into control and treatment groups. Each group contained 10 animals. Diameters of the tumor masses (subcutaneous) were measured weekly with a caliper. Volumes of the masses were calculated as tumor volume $(mm^3) = (width)^2 \times (length) \times 0.5$ [26]. Daily infiltrative injections into the established tumor masses were carried out with 10 and 30 μg contortrostatin in 0.1 ml of 0.9% NaCl over a period of 6 weeks. An equal volume of 0.9% NaCl was injected into control animals.

Immunohistochemical analyses. Tumor masses were processed by fixing in phosphate buffered 10% formalin, embedded in paraffin, sectioned at 4 μm, and tissue sections processed for immunohistochemistry, including antigen-retrieval. Immunohistochemical stains were carried out using monoclonal anti-Factor VIII-related antigen antibody and a detection kit from Zymed Laboratories . Immunohistochemistry staining was performed according to an established protocol provided by the manufacturer. Hematoxylin and eosin stains were used for histopathologic correlation. Image analysis and quantitation employed a Leica Q570 image analyzer to determine the area (pixels) of stained vessels in selected fields (880 μ diameter; 0.61 mm^2) from tumor sections at 200× magnification. Field selection for measurements of intratumoral microvessel density focused on 'hot spots' of high vessel density and excluded areas of tumor necrosis. Quantitation follows the guidelines described elsewhere [27], and was performed in a blind method.

Cell adhesion assay. Dulbecco's Modified Eagle Medium (DMEM) with 10% fetal bovine serum was employed for culture of HUVEC. Cells were incubated at 37 °C with 5% CO_2. Contortrostatin or extracellular matrix proteins were immobilized on Immulon-II 96-well microtiter plate (Dynex Technologies, Inc., Chantilly, Virginia) by incubating the protein, dissolved in phosphate-

buffered saline (PBS), on the plate overnight at 4 °C. The amount of ECM protein or contortrostatin supporting more than 90% cell adhesion was determined experimentally. In this study, the amount of contortrostatin, human fibronectin, or vitronectin immobilized were 0.1, 0.5, or 1 μg per well, respectively. Excess proteins were washed away with PBS. Unbound sites were blocked with 1% bovine serum albumin (BSA) in PBS. One hundred microlitres of HUVEC (5×10^5/ml) were seeded in the coated microtiter plate wells. The cells were treated with various reagents by incubation at 25 °C for 20 min prior to seeding. Seeded cells were allowed to adhere for 1 h at 37 °C. After unbound cells were washed away, the extent of cells adhesion was determined by CellTiter 96^{TM} AQ_{ueous} Non-Radioactive Cell Proliferation Assay kit (Promega, Madison, Wisconsin). The tests were performed in triplicate, and the assays were repeated at least three times to confirm results.

Cell invasion assay. Modified Boyden chambers were employed for this assay [28]. Twelve-well Transwell chambers (Corning Costar, Cambridge, Massachusetts) with 12 μm pores were coated with 150 μl of 1:50 diluted Matrigel in serum free medium. Coated wells were allowed to air dry in a sterile hood overnight and were rehydrated with serum free medium for 2 h at room temperature prior to use. HUVEC were mixed with various concentrations of contortrostatin or other inhibitors in serum free medium. The cells (2.5×10^5) were applied to the upper chambers of the Transwell and allowed to invade across the Matrigel-coated membrane for 6 h. Medium containing bFGF (20 ng/ml) as chemoattractant was added in the bottom well. After non-invaded cells were removed with wet cotton swabs, invaded cells attached to the bottom of the membrane were fixed and stained with Diff Quick^{TM} staining kit (Dade Diagnostics of P. R. Inc., Aguada, Puerto Rico). The number of invaded cells were quantitated microscopically by finding the mean cell number of three randomly selected high power vision fields. Experiments were performed in duplicate, and the assays were repeated to verify results.

Angiogenesis assay on chick embryo chorioallantoic membrane (CAM). Ten-day-old chick embryos were purchased from a local poultry farm (AA Labs, Westminster, California). The embryos were incubated at 37 °C with 60% humidity. Preparation of the CAM was described in detail elsewhere [29]. To grow tumor masses, 1×10^7 MDA-MB-435 cells in 30 μl of PBS were applied on the CAM. After 7 days, the tumor masses and surrounding CAM were cut out. For the angiogenesis assay, growth factor (200 ng) impregnated filter discs or carefully trimmed tumor masses (about 10 mg each) were transplanted on freshly prepared 10-day-old CAMs. Contortrostatin treatment, either i.v. injection or topical administration, was performed 24 h after transplantation. CAM around the filter discs or tumors were cut off 48 h after treatment, and angiogenesis on the inner side of the CAM was examined under stereomicroscope and documented photographically. Quantitation of angiogenesis was carried out by determination of the number of blood vessel branch points within the confined region of the filter disc. The number of branch points is relative to the number of newly sprouting angiogenic vessels [29]. The counting was performed with 250× magnification, and the stereomicroscope was maintained in a single focal plane.

Competitive binding assay. HUVEC harvested from subconfluent flasks were resuspended in 1% BSA/PBS at density of 1×10^7/ml and aliquoted 100 μl per tube. Cells were incubated with contortrostatin of different concentrations at room temperature for 30 min, followed by addition of 5 μg/ml 7E3, 10E5, or LM609. Incubations were continued for another 30 min. The cells were washed twice and resuspended in 1% BSA/PBS. Goat anti-mouse IgG conjugated with FITC was added to the suspension at a final titer of 1:200. After 30 min incubation at room temperature in darkness, unbound FITC-conjugated IgG was washed off, and the fluorescent intensity of the cells was analyzed using flow cytometry (FACScan, Becton Dickinson, Bedford, Massachusetts). Tests were performed in duplicate and the experiment was repeated three times.

Competitive binding of contortrostatin with ^{125}I-c7E3 Fab. Fifty microlitres of purified $\alpha v\beta 3$ or $\alpha IIb\beta 3$ (0.5 μg/ml) was used to coat 96-well polystyrene Immulon Removawell plates (Dynex Technologies, Chantilly, Virginia) overnight at 4 °C. A series of dilutions of contortrostatin was prepared in HEPES buffered saline containing 1 mM $CaCl_2$ and 1 mM $MgCl_2$. Dilutions of contortrostatin were added to plates simultaneously with ^{125}I-c7E3 Fab (approximately 2 μCi/μg, 1 μg/ml final concentration) and incubated for 1 h at 37 °C. The plates were washed, and wells were removed for radioactivity counting with a gamma counter. Data is presented as percent of maximal ^{125}I-c7E3 Fab bound in the absence of contortrostatin.

Apoptosis assay. HUVEC (6×10^5 cells) were incubated in the presence or absence of contortrostatin for 20 min at room temperature prior to applying to 6-well plates coated with either vitronectin (5 μg/ml), fibronectin (2.5 μg/ml), or contortrostatin (2.5 μg/ml). After 18 to 20 h incubation at 37 °C, cells were collected and smeared on poly-lysine coated slides. The slides were stained using TdT-mediated dUTP nick-end labeling (TUNEL) method [30]. Staining is performed using Apoptosis Detection System, Fluorescence^{TM} kit (Promega, Madison, Wisconsin). Slides were examined by fluorescence microscopy. DNA fragmentation was also analyzed by electrophoresis on 1.5% agarose gel using DNA extracted from HUVEC samples. The method used to extract fragmented DNA is described elsewhere [31].

Results

Contortrostatin inhibits growth of human breast cancer in a nude mouse model. An orthotopic xenograft metastatic model of human breast cancer in nude mice was established by implantation of MDA-MB-435 cells in the mammary fat pads of 4-week-old female nude mice as previously described [25]. Palpable tumors appeared 10 days after implantation. Without therapeutic intervention, the implanted tumors grew to about 1 cm^3 in 8 weeks. Local injection of contortrostatin (10 and 30 μg/mouse/day) was started on the 14th day post-implantation when the tumor take was confirmed by a subcutaneous palpable mass (designated as 'week 0' of injection, Figure 1). Equal volume of 0.9% NaCl was injected in the control group of animals. Weekly measurements of tumor volume during treatment showed that local injection of contortrostatin substantially inhibited the growth rate of the tumor, and this inhibitory effect is dose-dependent (Figure 1). Typical appearance of the tumors in the control group showed high nodularity in addition to their large size. In comparison, tumors in the treated group had a smoother surface and much smaller size (Figure 2). No side-effects (e.g., internal bleeding) were observed, suggesting that contortrostatin was well tolerated.

Contortrostatin inhibits angiogenesis induced by bFGF and VEGF in CAM. VEGF and bFGF, expressed by multiple malignant cell lines, have been well documented as specific and potent endothelial mitogens and chemoattractants [32, 33]. We tested whether contortrostatin blocks angiogenesis induced by VEGF and bFGF using the CAM assay. Contortrostatin was given topically on filter discs applied to the CAM 24 h after application of the growth factors and angiogenesis was determined 48 h later. Figure 3 presents a series of typical results that demonstrated that contortrostatin (5 μg/embryo) effectively inhibited angiogenesis induced by bFGF and VEGF. Figures 3C and F show that contortrostatin treatment after VEGF and bFGF, respectively, abruptly stopped capillary development. Patchy hemorrhagic spots can be seen on the white background in both contortrostatin-treated filter discs. The bleeding is typical in the contortrostatin treated discs using 5 μg contortrostatin, presumably due to the disformity and leakage of the capillary. Vessels that developed prior to contortrostatin treatment were not altered, indicating that contortrostatin only blocks angiogenic vessel. Quantitation of angiogenesis in these CAM models demonstrated that contortrostatin treatment significantly reduces angiogenesis induced by both angiogenic factors ($P < 0.05$) (Figure 4).

Contortrostatin inhibits angiogenesis induced by MDA-MB-435 tumor in CAM. We employed the CAM to test if the inhibitory effect of contortrostatin on breast cancer progression is partially due to its antiangiogenic effect. These CAM models were treated on day 2 post-transplantation with contortrostatin by either i.v. injection (125 ng/embryo) or topical administration (1 μg/embryo). Representative results are illustrated in Figure 5. In the control CAM (Figures 5A and C, saline treated), numerous blood vessels growing around and into the tumors were visible. The results clearly showed that both systemic and topical administration of contortrostatin significantly inhibited angiogenesis induced by the transplanted tumors (Figures 5B and D). Similar to the results presented in Figure 3, vessels already existing before contortrostatin treatment were not affected. In these studies only 1 μg of contortrostatin was used for treatment and the patchy hemorrhagic spots were not observed. These hemorrhagic regions may, therefore, represent a dose-related phenomenon since in the VEGF and bFGF studies 5 μg of contortrostatin was used.

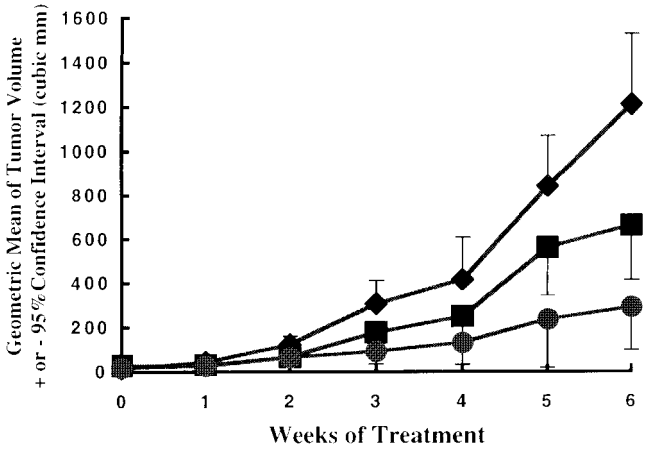

Figure 1. Effect of contortrostatin on the growth of MDA-MB-435 tumor in experimental nude mice. MDA-MB-435 (5×10^5) cells were implanted into mammary fat pads of 4-week old female nude mice. Palpable tumor masses appeared around the 14th day post-implantation. Daily local injection of contortrostatin was initiated on the 14th day post-implantation. The volumes of tumor masses (geometric mean $\pm$ 95% confidence interval) of control (◆) and contortrostatin-treated group (10 μg/mouse/day, ■; 30 μg/mouse/day, ●) are shown. Each group contains 10 animals.

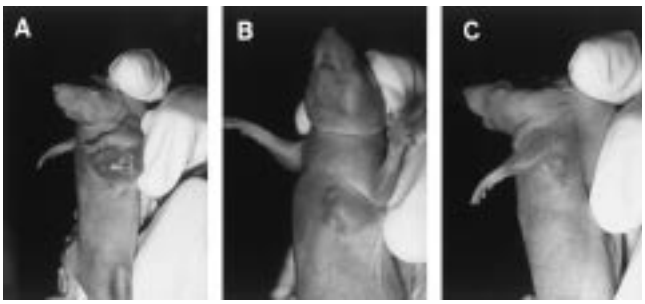

Figure 2. Typical tumor growth in experimental nude mice. (A) Representative tumor in mouse of control group (treated with normal saline). Typical appearance of the tumors in the control group showed a high degree of nodularity in addition to their large size. (B) Reduction of tumor size in the group of mice treated with low dose of contortrostatin by local injection. (C) Significantly reduced tumor size in mice treated with high dose of contortrostatin. Tumors in the treated group had a smoother surface and much smaller size.

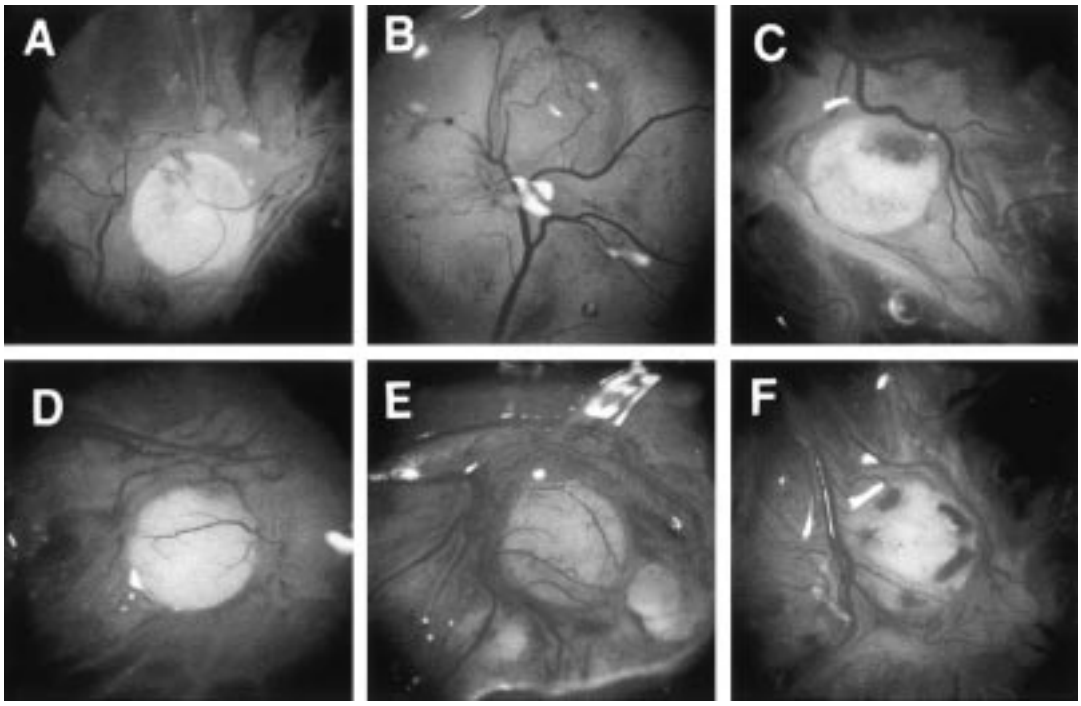

Figure 3. Contortrostatin inhibits angiogenesis induced by angiogenic factors in CAM models. The CAM models were prepared using 10-day-old chick embryos (see details in Materials and methods). (A) and (D) Negative control CAM with blank filter discs; (B) Positive control CAM with filter paper disc containing 200 ng bFGF alone; (C) CAM treated with bFGF and contortrostatin (5 μg); (E) Positive control CAM with filter paper disc containing 200 ng VEGF alone; (F) CAM treated with VEGF and contortrostatin (5 μg). Angiogenesis induced by both growth factors was significantly inhibited by contortrostatin. Each group contained 5 to 6 CAMs and the experiment was repeated three times. Representative results from multiple experiments are shown.

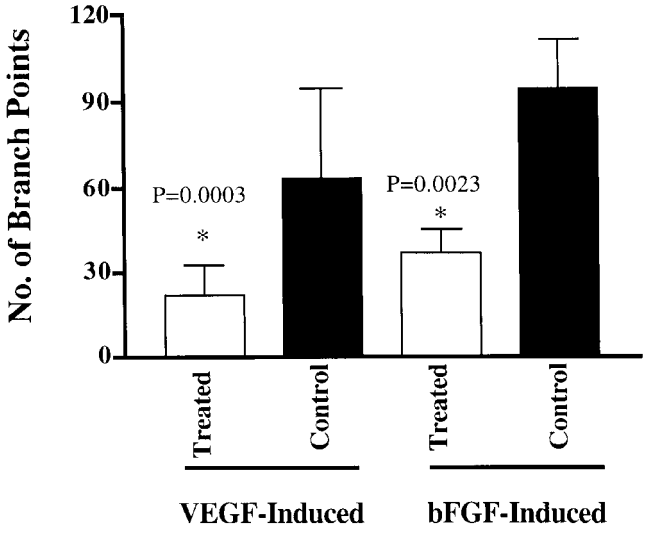

Figure 4. Quantitation of angiogenesis reduction in CAM models treated by contortrostatin. Angiogenesis was quantitated by the number of blood vessel branch points within the confined region of the filter disc. The number of branch points is relative to the number of newly sprouting angiogenic vessels. The counting was performed with 250× magnification, and the stereomicroscope was maintained at one focal plane. The results demonstrated that contortrostatin treatment significantly reduces angiogenesis induced by both VEGF and bFGF.

Contortrostatin inhibits angiogenesis induced by human breast cancer in a nude mouse model. To quantify angiogenesis in the nude mouse breast cancer model, the angiogenic vascular endothelial cells in the tumor tissues were stained by an immunohistochemical method using an antibody to factor VIII-related antigen. Areas occupied by the stained vascular endothelial cells in the 'hot spot' were quantitated. Figure 6 shows that the area of stained cells per 'hot spot' was significantly reduced in contortrostatin-treated samples. This reduction seems to have a dose–response relationship with contortrostatin.

Contortrostatin inhibits the adhesion of HUVEC to ECM proteins. We chose HUVEC to investigate the effect of contortrostatin on the interaction of vascular endothelium with the ECM. Different ECM proteins were immobilized on the bottom of 96-well plates. Contortrostatin was examined for its ability to inhibit adhesion of HUVEC to immobilized ECM proteins. Figure 7 demonstrates that contortrostatin inhibits adhesion of HUVEC to immobilized vitronectin (IC_{50} approximately 3 nM). However, at the concentrations examined, it is not an effective inhibitor of adhesion of HUVEC to fibronectin and Matrigel.

Competetive binding assays. αIIbβ3 is the specific binding site for contortrostatin on human platelets [23]. Since αIIbβ3 and αvβ3 share β-chain homology and contortrostatin blocks the adhesion of HUVEC to immobilized vitronectin, we determined whether contortrostatin binds to the vitronectin receptor αvβ3 on HUVEC [34]. Using flow cytometry, we were able to

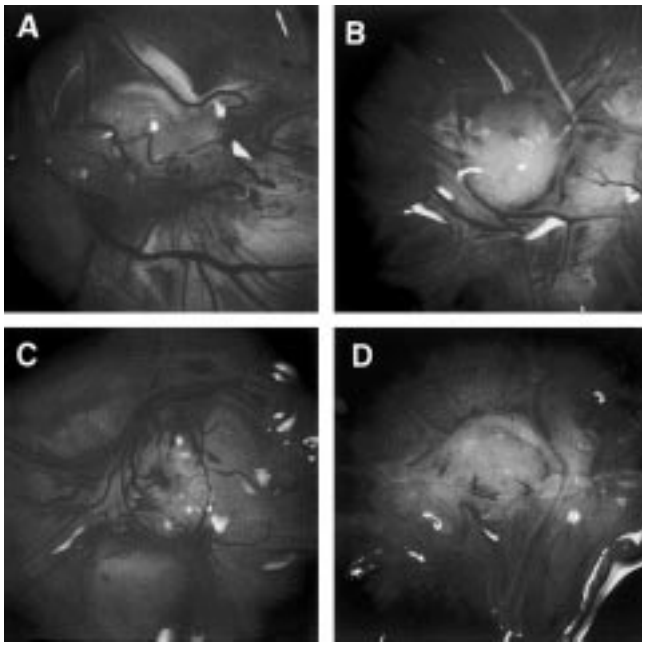

Figure 5. Contortrostatin inhibits angiogenesis induced by breast cancer in CAM models. Tumor mass (~10 mg) was transplanted onto a 11-day-old chick embryo (see details in 'Materials and methods'). (A) CAM around MDA-MB-435 tumor, topically treated with normal saline (control); (B) CAM around tumor, topically treated with 1 μg of contortrostatin; (C) CAM around tumor after i.v. injection of 100 μl normal saline (control), and (D) CAM around tumor after i.v. injection of 125 ng contortrostatin in 100 μl normal saline. Both topical and systemic administration of contortrostatin significantly inhibited angiogenesis induced by MDA-MB-435 cells. Each group contained 5 to 6 CAMs and the experiment was repeated three times. Representative results from multiple experiments are shown.

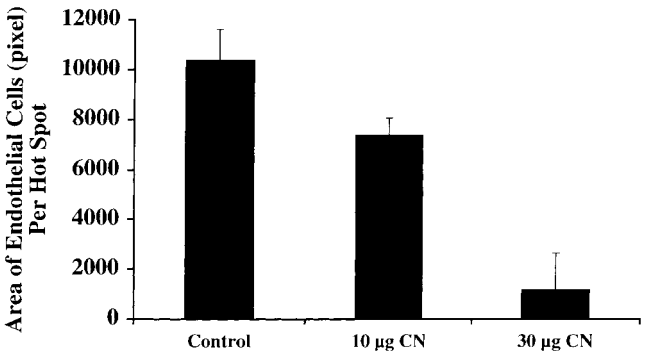

Figure 6. Contortrostatin inhibits angiogenesis induced by human breast cancer in nude mouse models. Immunohistochemical stains were carried out on mammary tumor tissue removed from the nude mouse model. Angiogenic vascular endothelial cells were probed by a monoclonal antibody against Factor VIII-related antigen. Image analyses determines the area (pixels) of stained vessels in selected 'hot spots' at 200× magnification.

detect LM609, monoclonal antibody (mAb) against $\alpha v\beta 3$ [35], binding to HUVEC, indicating that integrin $\alpha v\beta 3$ is expressed on HUVEC. 7E3 is a mAb against $\alpha IIb\beta 3$ [36], which is mainly expressed in platelets and megakaryocytes [37]. However, 7E3 also cross-reacts with $\alpha v\beta 3$ [38]. FACS analysis indicates that 7E3 binds

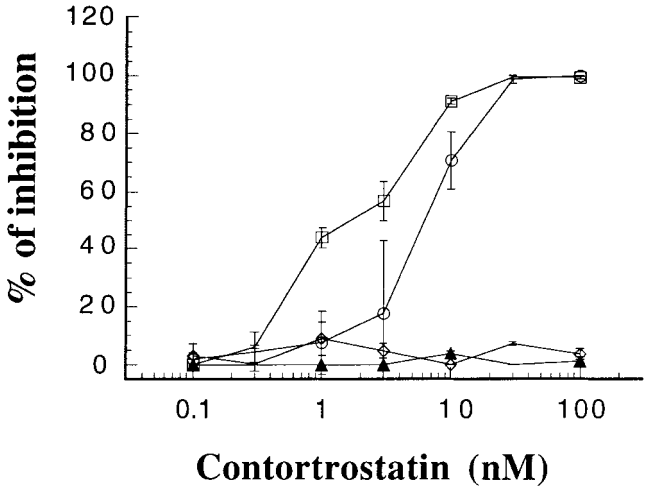

Figure 7. Contortrostatin inhibits adhesion of HUVEC to immobilized vitronectin. Contortrostatin inhibits adhesion of HUVEC to immobilized vitronectin (1 μg/well) (squares) and contortrostatin (0.1 μg/well) (circles), but not to fibronectin (0.5 μg/well) (diamonds) or Matrigel (1:100) (solid triangles). Each point is the mean absorbance of triplicate wells ±SD. Experiment was repeated 3 times.

to HUVEC (Figure 8A), and contortrostatin competes with 7E3 binding to $\alpha v\beta 3$ (Figure 8B). This competitive binding was not observed with LM609, because it apparently binds to a different epitope than contortrostatin. We did not detect binding of 10E5 to HUVEC (data not shown). 10E5 is a highly specific mAb to $\alpha IIb\beta 3$ [39] that does not cross-react with $\alpha v\beta 3$. This finding excluded the possibility that binding of contortrostatin to HUVEC was due to $\alpha IIb\beta 3$.

The interaction of contortrostatin with purified integrins was directly characterized using radiolabeled antibody and a cell-free binding system (Figure 9). Purified $\alpha IIb\beta 3$ and $\alpha v\beta 3$ were coated in the wells of 96-well plates. Contortrostatin was allowed to compete with ^{125}I-c7E3 Fab for binding to the immobilized integrins. Contortrostatin not only competed with 7E3 Fab for binding to $\alpha v\beta 3$, but it exhibited greater than 13-fold higher affinity to $\alpha v\beta 3$ ($IC_{50} = 0.35$ nM) than to $\alpha IIb\beta 3$ ($IC_{50} = 4.7$ nM).

Contortrostatin inhibits invasion of HUVEC. The effect of contortrostatin on invasion of HUVEC was investigated using Matrigel-coated Boyden chambers. Basic FGF (20 ng/ml) in the lower chamber strongly induced the migration of HUVEC, whereas, pretreatment of HUVEC with contortrostatin (0.5 μM) effectively prevented invasion (Figure 10). It is worthwhile to note that while the invasion of HUVEC was inhibited, adhesion of these cells to the Matrigel-coated filter was not affected. Therefore, the observed inhibitory effect of contortrostatin on HUVEC is most likely due to the suppression of cellular motility instead of prevention of adhesion. Pretreatment of HUVEC with 7E3 (200 μg/ml) does not prevent the cells from adhering to the Matrigel-coated filter. However, it does inhibit invasion of HUVEC as shown in Figure 10, suggesting that

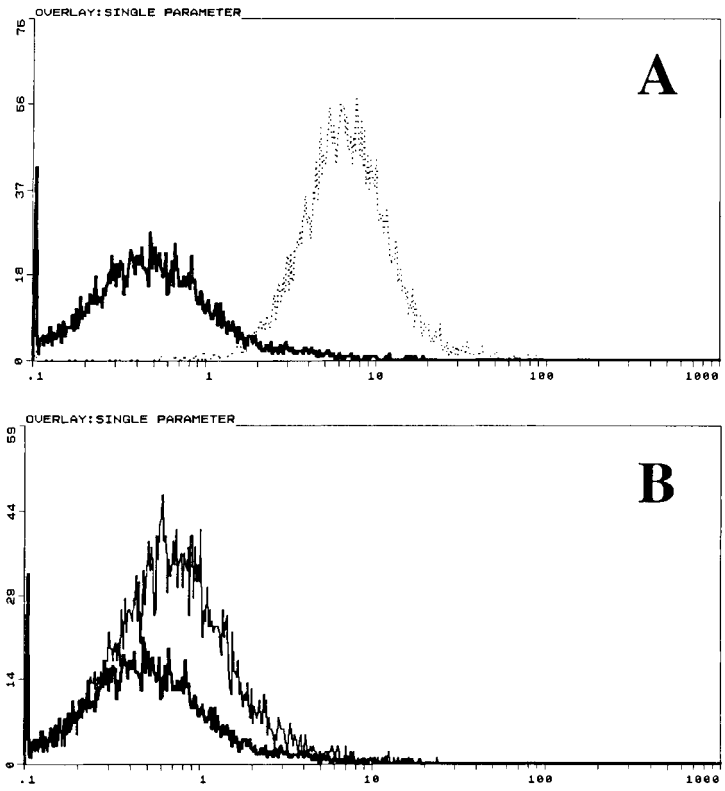

Figure 8. Contortrostatin specifically inhibits binding of 7E3 to $\alpha v\beta 3$ in HUVEC. This figure shows the binding of antibodies to HUVEC integrins as detected by flow cytometry. (A) 7E3 (5 μg/ml), a mAb to $\alpha IIb\beta 3$ which also cross reacts with $\alpha v\beta 3$, binds to HUVEC; (B) Contortrostatin (1 μM), added 20 min prior to addition of 7E3, effectively inhibits binding of 7E3. The lower peak represents the background, while the higher peak is the experimental.

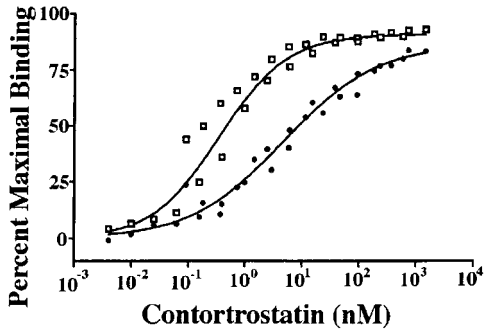

Figure 9. The affinity of contortrostatin to $\alpha v\beta 3$ is higher than that to $\alpha IIb\beta 3$. Purified integrins (2.5 ng) were immobilized in 96-well plate and competitive inhibition by contortrostatin of ^{125}I-7E3 Fab binding was measured. Contortrostatin inhibits binding of ^{125}I-7E3 Fab to both $\alpha v\beta 3$ (squares) and $\alpha IIb\beta 3$ (circles). The data points shown are from three separate experiments normalized and graphed together. Non-linear regression of the combined data indicated that the inhibitory potency of contortrostatin with $\alpha v\beta 3$ ($IC_{50} = 0.35$ nM) is more than 13-fold higher than with $\alpha IIb\beta 3$ ($IC_{50} = 4.7$ nM).

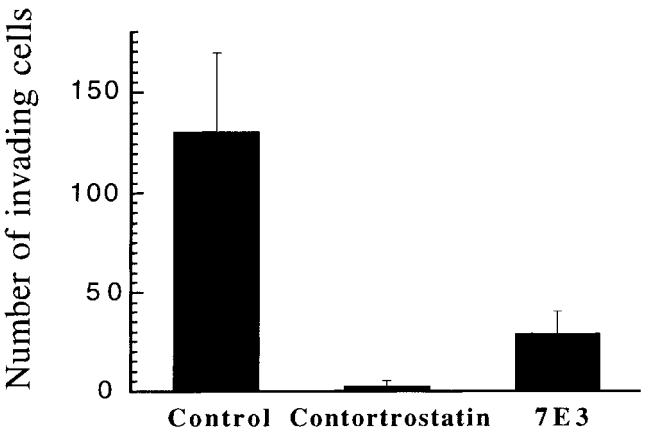

Figure 10. Both contortrostatin and 7E3 inhibit invasion of HUVEC through Matrigel. HUVEC pretreated with contortrostatin (0.5 μM) or 7E3 (200 μg/ml) were allowed to invade through the Matrigel-coated Boyden chamber. Basic FGF (20 ng/ml) served as chemoattractant in the lower chamber. 7E3 inhibits invasion by approximately 75%, while contortrostatin completely blocks invasion. The means of duplicate experiments are presented, error bars indicate SD.

functional blockade of integrin $\alpha v\beta 3$ inhibits HUVEC motility.

Detachment of HUVEC from immobilized vitronectin induces apoptosis. Endothelial cells are anchorage-dependent, detachment from their anchorage site results in apoptosis [31, 40]. We determined whether detachment of HUVEC from a vitronectin-coated surface by contortrostatin causes apoptosis. In the initial studies, we analyzed DNA fragmentation, a marker of apoptosis, using electrophoretic analysis of DNA isolated from HUVEC. As shown in Figure 11, DNA fragmentation was not detected in HUVEC 18–20 h after plating on a vitronectin-coated surface. Contortrostatin-treated HUVEC did not adhere to vitronectin-coated plates and DNA fragmentation was obvious in these cells

after 18–20 h. The fragmentation pattern is similar to that observed by Meredith et al. in a similar experiment [31], and was observed only in cells detached from immobilized vitronectin by contortrostatin (Figure 11A). Importantly, DNA fragmentation was not detected in HUVEC following 18–20 h of adhesion to immobilized contortrostatin. These findings were confirmed by additional studies using the TUNEL method, which stains the 3′-end of fragmented DNA. DNA fragmentation was observed by this method in HUVEC detached from vitronectin by pre-treatment with contortrostatin (500 nM) (Figure 11C). No fragmentation of DNA was detected in cells which adhered either to a vitronectin-coated surface (Figure 11B), or to contortrostatin.

Discussion

The hypothesis that tumor growth is angiogenesis dependent [1] has become dogma. Folkman [41] proposed a two-compartment tumor model composed of vascular endothelial cell and tumor cell compartments. Tumor cells can stimulate the proliferation and migration of endothelial cells by producing angiogenic factors. On the other hand, endothelial cells can promote tumor growth by secretion of various cytokines [41]. The paracrine effect, together with blood perfusion supplied by angiogenesis, promotes growth and metastasis of the tumor. In the context of the two-compartment model, it is obvious that antiangiogenic therapy could be a potentially effective mechanism to control cancer progression.

Our findings reported herein indicate that the dimeric disintegrin contortrostatin is a potent inhibitor of angiogenesis both *in vitro* and *in vivo*. To elucidate the mechanism of action, we found that the vitronectin receptor, integrin $\alpha v\beta 3$, is a target for contortrostatin. The importance of vitronectin receptors in a number of physiological and pathological processes has received increasing attention. The expression of $\alpha v\beta 3$ was significantly up-regulated in vascular endothelial cells in wound-repairing granulation tissue [12], tumor implantation sites in animals [42] on bFGF treated CAMs [13], and vasculogenic tissue [11]. This integrin is not detectable in the dermis and epithelium of normal skin [7]. Integrins expressed on the surface of HUVEC include $\alpha 2\beta 1$, $\alpha 3\beta 1$, $\alpha 5\beta 1$, $\alpha 6\beta 1$, $\alpha v\beta 1$, and $\alpha v\beta 3$ [43]. Among these, $\alpha 5\beta 1$, and $\alpha v\beta 3$ are well-established RGD recognition integrins [44]. Interestingly, not all disintegrins interact with $\alpha v\beta 3$. Having screened seven disintegrins, Juliano et al. [18] found only echistatin and kistrin potently inhibited the binding of mAb 7E3 to HUVEC. Recently, triflavin [19] and accutin [20] were reported to bind to $\alpha v\beta 3$ as well. However, contortrostatin apparently has higher affinity to this integrin than other disintegrins. The evidence comes from the following experimental data. Although both contortrostatin and accutin compete with 7E3, contortrostatin completely blocks binding of 7E3 at a concentration of 1 μM, whereas at 2 μM, accutin only inhibits about 80% of 7E3 binding [20]. To inhibit adhesion of HUVEC to immobilized vitronectin, the IC_{50} for contortrostatin is about 3 nM, whereas those for accutin and triflavin are about 200 and 180 nM, respectively.

Although disintegrins including contortrostatin bind to the fibronectin receptor $\alpha 5\beta 1$, we report here that contortrostatin did not block adhesion of HUVEC to fibronectin coated plates (Figure 7). This phenomenon was also found by Juliano et al. with kistrin and echistatin [18]. In contrast, both triflavin and accutin inhibit adhesion of HUVEC to fibronectin [19, 20]. The reason for this distinction in integrin binding specificity among the disintegrins is not known at this time.

The *in vivo* survival of vascular endothelial cells depends on their attachment and spreading on appropriate ECM

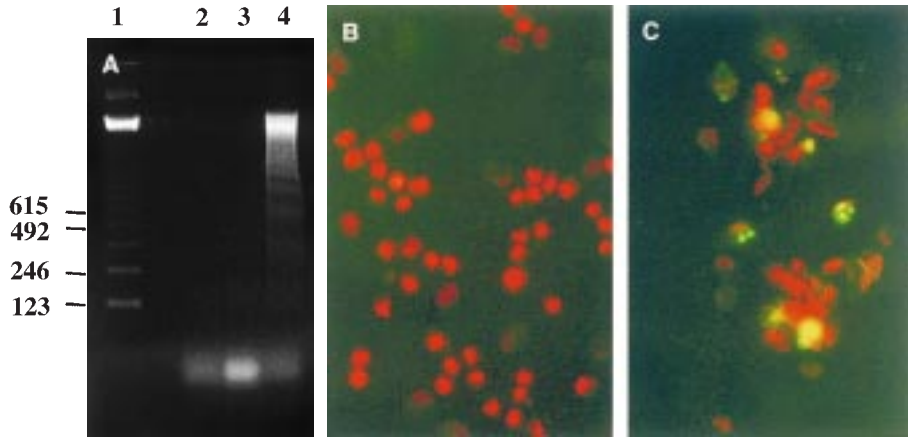

Figure 11. Contortrostatin induces HUVEC apoptosis. (A) HUVEC were seeded on contortrostatin-coated (5 μg) (lane 2) 30 mm-plate, as well as vitronectin-coated (2.5 μg) plate in the absence (lane 3) or presence (lane 4) of contortrostatin (500 nM). Nuclear extracts from these cells were separated on 1.5% agarose gel. DNA fragmentation was only found in HUVEC treated with contortrostatin which were detached from immobilized vitronectin, as shown in lane 4. DNA ladder (123 bp) was loaded in lane 1. (B) Fluorescence microscopy shows control HUVEC (attached to immobilized vitronectin) with intact nuclei, both cytoplasm and nuclei are stained by propidium iodide (red). (C) shows fluorescein-labeled DNA fragmentation (green) in contortrostatin (500 nM) treated HUVEC. These results are representative of three identical experiments.

proteins. Meredith et al. [31], reported that apoptosis was blocked by plating endothelial cells on immobilized integrin $\beta 1$ antibody suggesting that integrin-mediated signals are required for maintaining viability of vascular endothelial cells. Contortrostatin prevented HUVEC from attaching to vitronectin; 18 h after contortrostatin treatment, DNA fragmentation was detected. Although similar results were reported with accutin [20], it is not known if binding of disintegrin to $\alpha v\beta 3$ alone elicits apoptosis of the cells. To answer this question, we tested the DNA from cells that adhered to immobilized contortrostatin. Since DNA fragmentation was not observed in HUVEC that attached to immobilized contortrostatin, our findings suggest that detachment *per se* is responsible for transition to the apoptotic state. Our observations agree with the findings of Stromblad et al. [14] that binding of HUVEC to immobilized LM609 suppressed apoptosis of these cells. We conclude, therefore, that ligation of HUVEC integrins, specifically $\alpha v\beta 3$, by contortrostatin does not induce apoptosis. Rather, it is the disruption of integrin–matrix interaction that impairs cell viability.

Contortrostatin inhibits invasion of HUVEC through Matrigel, which is predominantly a laminin matrix. It is noteworthy that contortrostatin treatment of HUVEC deprived the cells of their motility although they retained their adhesiveness to ECM proteins other than vitronectin. Sheu et al. [19] also reported that high concentration of laminin (2 μg per well) support significant attachment of HUVEC, and this adhesion is not blocked by the disintegrin triflavin. Triflavin was not tested in Matrigel-coated Transwell invasion chamber. However, in chambers coated with fibronectin and vitronectin, the concentration of triflavin required to inhibit HUVEC migration is higher than that of contortrostatin tested in Matrigel-coated chamber. 7E3 had no effect on endothelial cell adhesion to ECM proteins other than vitronectin, but it was also able to inhibit HUVEC invasion, suggesting that blockage of $\alpha v\beta 3$ in this system results in immobilization of HUVEC. The role of integrin $\alpha v\beta 3$ in cell invasion involves more than just adherence to vitronectin. Clyman et al. [45] showed that cell adhesion to fibronectin, laminin, and types I and IV collagen depended exclusively on functioning $\beta 1$ integrins, whereas cell migration over these substrates depended to a large extent on the $\alpha v\beta 3$ integrin. Earlier investigations clearly showed that overexpression of $\alpha v\beta 3$ in carcinoma cells correlated with invasiveness [46–48]. Basic fibroblast growth factor (bFGF) induces an initial wave of mitogen-activated protein (MAP) kinase followed by sustained increase of enzyme activity in endothelial cells. The sustained wave of MAP kinase activity can be blocked by an antagonist of $\alpha v\beta 3$ [49]. Cheresh and colleagues recently showed that the ras/MAP kinase signal transduction pathway leads to phosphorylation and activity enhancement of myosin light chain kinase (MLCK). MLCK in turn induces phosphorylation of myosin light chain(s) providing the cells with locomotion by regulating myosin/actin interaction [50]. Thus, it is reasonable to postulate that, as an antagonist of $\alpha v\beta 3$, contortrostatin inhibits HUVEC motility as well as adhesion to vitronectin.

Although the antiangiogenic activity of triflavin, accutin and salmosin have been tested in the CAM model [19–21], until recently it was not known if disintegrins are therapeutically effective in inhibiting tumor growth in any vertebrate animal cancer model [21]. In the present study, we tested contortrostatin in an orthotopic human breast cancer model in nude mice. The orthotopic model maximizes the similarity to the clinical situation regarding the interaction between breast cancer and its microenvironment during angiogenesis. This is the first study of the use of an antiangiogenic disintegrin in an orthotopic animal tumor model, and the results suggest that local injection of contortrostatin can significantly reduce angiogenesis and the growth rate of the tumors. In addition, the chronic (6-week-long) treatment with contortrostatin suggests that it is well tolerated when delivered through the parenteral route.

Conclusion

Contortrostatin is a novel and potent inhibitor of angiogenesis. It appears to block several critical steps in neovascularization, and inhibits angiogenesis induced by multiple factors, including VEGF and bFGF, in the CAM model. In nude mice in which mammary fat pads were injected with MDA-MB-435 human mammary carcinoma cells, daily injection of contortrostatin into the established tumors inhibits angiogenesis and tumor growth in a dose-dependent manner. Dosages up to 30 μg/mouse/day are well tolerated. Integrin $\alpha v\beta 3$ is identified as the binding site of contortrostatin on vascular endothelial cells. The inhibition of angiogenesis caused by contortrostatin is probably the sum of several mechanisms. First, blockade of $\alpha v\beta 3$ prevents adhesion of vascular endothelial cells to vitronectin; this in turn elicits survival signal conflict and induces apoptosis of the vascular endothelial cells. Second, contortrostatin inhibits HUVEC mobility by interfering with the normal function of $\alpha v\beta 3$. Further studies on contortrostatin may lead to the development of a potent antiangiogenic agent with clinical potential for cancer therapy.

Acknowledgements

The authors would like to thank Patricia Sassoli of Centocor for her expert technical assistance. We would also like to acknowledge the Flow Cytometry Laboratory of the University of Southern California for performing FACS analysis. Gratitude is extended to Drs Florence Hofman, David Cheresh, Janet Price and Centocor, Inc. for sharing their valuable material. Appreciation is also due to Drs Russell P. Sherwin and Valda Richters for assistance in image analysis, to

Drs Vijay Kalra and Yamin Shen for consultations in HUVEC culture technique, and to Dr Peter Brooks for discussion on analysis of angiogenesis.

This work was supported by funds from the California Breast Cancer Research Program of the University of California, Grant Number 1RB-0052 (to F.S.M.). Q. Z. is a recipient of Postdoctoral Fellowship from the California Breast Cancer Research Program of University of California (3FB-0125), from the Susan G. Komen Breast Cancer Foundation (No. 9860), and Postdoctoral Fellowship Supplement Support from the University of Southern California/Norris Comprehensive Cancer Center.

References

1. Folkman J. Tumor angiogenesis: therapeutic implications. N Engl J Med 1971; 285: 1182–6.
2. Folkman J. Editorial: Angiogenesis and breast cancer. J Clin Oncol 1994; 12: 441–3.
3. Folkman J. Tumor Angiogenesis. In: Holland JF, Bast RC, Morton DL, Frei III E, Kufe DW, Weichselbaum RR (eds) Cancer Medicine. Baltimore: Williams & Wilkins 1997; 181–204.
4. Hanahan D, Folkman J. Patterns and emerging mechanisms of the angiogenic switch during tumorigenesis. Cell 1996; 86: 353–64.
5. O'Reilly MS, Holmgren L, Chen C, Folkman J. Angiostatin induces and sustains dormancy of human primary tumors in mice. Nat Med 1996; 2: 689–92.
6. O'Reilly MS, Boehm T, Shing Y et al. Endostatin: An endogenous inhibitor of angiogenesis and tumor growth. Cell 1997; 88: 277–85.
7. Brooks PC, Montgomery AMP, Rosenfeld M et al. Integrin $\alpha v\beta 3$ antagonists promote tumor regression by inducing apoptosis of angiogenic blood vessels. Cell 1994; 79: 1157–64.
8. Dvorak HF, Brown LF, Detmar M, Dvorak AM. Vascular permeability factor/vascular endothelial growth factor, microvascular hyperpermeability, and angiogenesis. Am J Pathol 1995; 146: 1029–39.
9. Weidner N, Semple JP, Welch WR, Folkman J. Tumor angiogenesis and metastasis – correlation in invasive breast carcinoma. N Engl J Med 1991; 324: 1–8.
10. Stromblad S, Cheresh DA. Cell adhesion and angiogenesis. Trends Cell Biol 1996; 6: 462–8.
11. Drake CJ, Cheresh DA, Little CD. An antagonist of integrin $\alpha v\beta 3$ prevents maturation of blood vessels during embryonic neovascularization. J Cell Sci 1995; 108: 2655–61.
12. Clark RAF, Tonnesen MG, Gailit J, Cheresh DA. Transient functional expression of $\alpha v\beta 3$ on vascular cells during wound repair. Am J Pathol 1996; 148: 1407–21.
13. Brooks PC, Clark RA, Cheresh DA. Requirement of vascular integrin $\alpha v\beta 3$ for angiogenesis. Science 1994; 264: 569–71.
14. Stromblad S, Becker JC, Yebra B et al. Suppression of p53 activity and p21WAF1/CIP1 expression by vascular cell integrin $\alpha v\beta 3$ during angiogenesis. J Clin Invest 1996; 98: 426–33.
15. Miyashita T, Harigai M, Hanada M, Reed JC. Identification of a p53-dependent negative response element in the *bcl*-2 gene. Cancer Res 1994; 54: 3131–5.
16. El-Deiry WS, Harper JW, O'Connor PM et al. WAF1/CIP1 is induced in p53-mediated G1 arrest and apoptosis. Cancer Res 1994; 54: 1169–74.
17. McLane M, Marcinkiewica C, Vijay-Kumar S et al. Viper venom disintegrins and related molecules [Review]. Proc Soc Exp Biol Med 1998; 219(2): 109–19.
18. Juliano D, Wang Y, Marcinkiewicz C et al. Disintegrin interaction with $\alpha v\beta 3$ integrin on human umbilical vein endothelial cells: Expression of ligand-induced binding site on $\beta 3$ subunit. Exp Cell Res 1996; 225: 132–42.
19. Sheu JR, Yen MH, Kan YC et al. Inhibition of angiogenesis *in vitro* and *in vivo*: Comparison of the relative activities of triflavin, an Arg-Gly-Asp-containing peptide and anti-$\alpha v\beta 3$ integrin monoclonal antibody. Biochim Biophys Acta 1997; 1336: 445–54.
20. Yeh CH, Peng HC, Huang T-F. Accutin, a new disintegrin, inhibits angiogenesis *in vitro* and *in vivo* by acting as integrin $\alpha v\beta 3$ antagonist and inducing apoptosis. Blood 1998; 92(9): 3268–76.
21. Kang I-C, Lee Y-D, Kim D-S. A novel disintegrin salmosin inhibits tumor angiogenesis. Cancer Res 1999; 59: 3754–60.
22. Trikha M, De Clerk YA, Markland FS. Contortrostatin, a snake venom disintegrin, inhibits $\beta 1$ integrin-mediated human metastatic melanoma cell adhesion, and blocks experimental metastasis. Cancer Res 1994; 54: 4993–8.
23. Trikha M, Rote WE, Manley PJ et al. Purification and characterization of platelet aggregation inhibition from snake venoms. Thromb Res 1994; 73: 39–52.
24. Clark EA, Trikha M, Markland FS, Bruggs JS. Structurally distinct disintegrins contortrostatin and multisquamatin differentially regulate platelet tyrosine phosphorylation. J Biol Chem 1994; 269(35): 21940–3.
25. Price JE, Polyzos A, Zhang RD, Daniels LM. Tumorigenicity and metastasis of human breast carcinoma cell lines in nude mice. Cancer Res 1990; 50: 717–21.
26. Osborne CK, Hobbs K, Clark GM. Effect of estrogens and antiestrogens on growth of human breast cancer cells in athymic nude mice. Cancer Res 1985; 45: 584–90.
27. Gasparini G, Harris AL. Prognostic significance of tumor vascularity. In Teicher BA (ed): Antiangiogenic Agents in Cancer Therapy. Totowa: Humana Press 1999; 317–39.
28. Repesh LA. A new *in vitro* assay for quantitating tumor cell invasion. Invasion Metastasis 1989; 9: 192–208.
29. Brooks PC, Montgomery AMP, Cheresh DA. Use of the 10-day-old chick embryo model for studying angiogenesis. In Howlett AR (ed): Methods in Molecular Biology. Totowa: Humana Press 1999; 257–69.
30. Gavrieli Y, Sherman Y, Ben-Sasson SA. Identification of programmed cell death *in situ* via specific labeling of nuclear fragmentation. J Cell Biol 1992; 119: 493–501.
31. Meredith JE, Fazeli B, Schwartz MA. The extracellular matrix as a cell survival factor. Mol Biol Cell 1993; 4: 953–61.
32. Connolly DT, Heuvelman DM, Nelson R et al. Tumor vascular permeability factor stimulates endothelial cell growth and angiogenesis. J Clin Invest 1989; 84: 1470–8.
33. Ferrara N, Houck K, Jakeman L, Leung DW. Molecular and biological properties of the vascular endothelial growth factor family of proteins. Endocr Rev 1992; 13: 18–32.
34. Felding-Habermann B, Cheresh DA. Vitronectin and its receptors. Curr Opin Cell Biol 1993; 5: 864–8.
35. Wayner EA, Orlando RA, Cheresh DA. Integrins $\alpha v\beta 3$ and $\alpha v\beta 5$ contribute to cell attachment to vitronectin but differentially distribute on the cell surface. J Cell Biol 1991; 113: 919–29.
36. Coller BS, Peerschke EI, Scudder LE, Sullivan CA. A murine monoclonal antibody that completely blocks the binding of fibroinogen to platelets produces a thrombasthenic-like state in normal platelets and binds to glycoproteins IIb and/or IIIa. J Clin Invest 1983; 72: 325–38.
37. Phillips DR, Charo IF, Scarborough RM. GP IIb-IIIa: The responsive integrin. Cell 1991; 65: 359–62.
38. Charo IF, Bekeart LS, Phillips DR. Platelet glycoprotein IIb-IIIa like proteins mediate endothelial cell attachment to adhesive proteins and the extracellular matrix. J Biol Chem 1987; 262: 9935–8.
39. Peerschke EI, Coller BS. A murine monoclonal antibody that blocks fibrinogen binding to normal platelets also inhibits fibrinogen interactions with chymotrypsin-treated platelets. Blood 1984; 64: 59–63.
40. Frisch SM, Francis H. Disruption of epithelial cell-matrix interactions induces apoptosis. J Cell Biol 1994; 124: 619–29.
41. Folkman J. Tumor angiogenesis and tissue factor. Nat Med 1996; 2: 167–8.

42. Brooks PC, Stromblad S, Klemke R et al. Antiintegrin $\alpha v\beta 3$ blocks human breast cancer growth and angiogenesis in human skin. J Clin Invest 1995; 96: 1815–22.
43. Luscinskas FW, Lawler J. Integrins as dynamic regulators of vascular function. FASEB J 1994; 930: 929–38.
44. Hynes RO. Integrins: Versatility modulation, and signaling in cell adhesion. Cell 1992; 69: 11–25.
45. Clyman RI, Mauray F, Kramer RH. $\beta 1$ and $\beta 3$ integrins have different roles in the adhesion and migration of vascular smooth muscle cells on extracellular matrix. Exp Cell Res 1992; 200: 272–84.
46. Jacob K, Bosserhoff AK, Wach F et al. Characterization of selected strongly and weakly invasive sublines of a primary human melanoma cell line and isolation of subtractive cDNA clones. Int J Cancer 1995; 60: 668–75.
47. Kawahara E, Imai K, Kumagai S et al. Inhibitory effects of adhesion oligopeptides on the invasion of squamous carcinoma cells with special reference to implication of αv integrins. J Cancer Res Clin Oncol 1995; 121: 133–40.
48. Liapis H, Adler LM, Wick MR, Rader JS. Expression of $\alpha v\beta 3$ integrin is less frequent in ovarian epithelial tumors of low malignant potential in contrast to ovarian carcinomas. Human Pathol 1997; 28: 443–9.
49. Eliceiri BP, Klemke R, Stromblad S, Cheresh DA. Integrin $\alpha v\beta 3$ requirement for sustained mitogen-activated protein kinase activity during angiogenesis. J Cell Biol 1998; 140(5): 1255–63.
50. Klemke RL, Cai S, Giannini AL et al. Regulation of cell motility by mitogen-activated protein kinase. J Cell Biol 1997; 137(2): 481–92.